General Disclaimer

One or more of the Following Statements may affect this Document

- This document has been reproduced from the best copy furnished by the organizational source. It is being released in the interest of making available as much information as possible.

- This document may contain data, which exceeds the sheet parameters. It was furnished in this condition by the organizational source and is the best copy available.

- This document may contain tone-on-tone or color graphs, charts and/or pictures, which have been reproduced in black and white.

- This document is paginated as submitted by the original source.

- Portions of this document are not fully legible due to the historical nature of some of the material. However, it is the best reproduction available from the original submission.

NASA CR-132697

Advanced Technology Laboratories inc

NASA CR-132697

MAY 1975

ATL TR 213

AN IMPROVED SOURCE FLOW CHARACTERISTIC TECHNIQUE FOR THE ANALYSIS OF SCRAMJET EXHAUST FLOW FIELDS

By

P. Del Guidice & S. Dash

PREPARED FOR

NATIONAL AERONAUTICS AND SPACE ADMINISTRATION
LANGLEY RESEARCH CENTER
HAMPTON, VIRGINIA 23365

UNDER

CONTRACT NO. NAS1-13303

BY

ADVANCED TECHNOLOGY LABORATORIES, INC.
Merrick and Stewart Avenues
Westbury, New York 11590

INDEX

INDEX

LIST OF SYMBOLS

x	axial distance (X^*/L^*)
y	height of nozzle (y^*/L^*)
z	lateral extent of nozzle (z^*/L^*)
s	streamline distance (s^*/L^*)
n	distance normal to streamline (n^*/L^*)
h	mixture enthalpy (h^*/u_∞^2)
L^*	reference length (throat height - ft)
M	Mach number
m_i	molecular weight of i^{th} species
α_i	mass fraction of i^{th} species (frozen mixture)
NSP	number of species (frozen mixture)
P	pressure ($P^*/\rho_\infty u_\infty^2$)
q	velocity (q^*/u_∞)
T	temperature (T^*/T_∞)
ρ	density (ρ^*/ρ_∞)
H	stagnation enthalpy (H^*/u_∞^2)
ΔS	incremental entropy change
w	average molecular weight of mixture (frozen mixture - w^*/w_∞)
Φ	fuel to air equivalence ratio (equilibrium mixture)
θ	flow inclination
Γ	equilibrium isentropic exponent
γ	ratio of specific heats (frozen mixture)
C_v	heat capacity at constant volume
μ	Mach angle

SECTION I
INTRODUCTION

The process of designing a nozzle for a hypersonic airbreathing vehicle involves a complex study of the inter-relationship among many parameters, i.e., internal-external expansion, vehicle lift, drag, pitching moments, structural and weight limitations. Reference (1) summarizes the various stages of the design process, wherein a range of design parameters are chosen via a simplified analysis described in Reference (2) with more sophisticated calculations performed after the range of parameters has been reduced. The second stage of the design procedure (i.e., a more sophisticated analysis) is described in Reference (3) and in this report.

As discussed below the source flow characteristic approach described in Reference (3) has been extended and improved. An improved streamline interpolation procedure has been incorporated. In addition, all characteristic and boundary calculations have been made compatible with frozen, equilibrium and ideal gas thermodynamic options, while slip surface calculations (cowl interaction) have been extended to underexpanded flow conditions.

Since viscous forces can significantly influence vehicle forces, pitching moments and structural/weight considerations a local integration via flat plate boundary layer skin friction and heat transfer coefficients has been included. These effects are calculated using the Spalding and Chi method described in Reference (7). All force and moment calculations are performed via integration of the local forces acting on the specified vehicle wetted areas.

While this report discusses in detail the improvements mentioned above, summaries of appropriate parts of Reference (3) have been included for purposes of clarity and continuity. Additional details may be found in Reference (3).

SECTION II
BASIC EQUATIONS

A. Equations of Motion - The equations governing the two dimensional, axisymmetric, or axially expanding inviscid flow of a gas mixture in chemical or frozen equilibrium may be written as follows:

Continuity: $$\frac{\partial}{\partial s}(\rho q) + \rho q \frac{\partial \theta}{\partial n} + J_1 \rho q \frac{\sin\theta}{y} + J_2 \rho q \frac{\cos\theta}{x} = 0 \qquad (1)$$

S-Momentum: $$\rho q \frac{\partial q}{\partial s} + \frac{\partial p}{\partial s} = 0 \qquad (2)$$

N-Momentum: $$\rho q^2 \frac{\partial \theta}{\partial s} + \frac{\partial p}{\partial n} = 0 \qquad (3)$$

Along a streamline the following relations are valid:

Conservation of Stagnation Enthalpy: $$\frac{\partial H}{\partial s} = 0 \quad \text{where } H = h + \frac{1}{2} q^2 \qquad (4)$$

Constancy of Equivalence Ratio: $$\frac{\partial \Phi}{\partial s} = 0 \quad \text{(equilibrium Mixture)} \qquad (5a)$$

or

Species Conservation: $$\frac{\partial \alpha_i}{\partial s} = 0 \quad (i=1, NSP) \text{ (Frozen Mixture)} \qquad (5b)$$

and the

Equation of State: $$p/\rho^{\Gamma} = \text{constant} \cdot \exp(-\Delta S/Cv) \qquad (6)$$

However for a frozen or equilibrium gas mixture $(\Delta S/Cv)$ along streamlines is zero in regions of continuous flow.

B. Thermodynamic State

Equilibrium Mixture - The static properties are defined via curve fits described in Reference (3) i.e.,

$$h = h\ (P,\phi,T) \qquad \text{static enthalpy} \qquad (7a)$$

$$\Gamma = \Gamma\ (P,h,\phi) \qquad \text{equilibrium isentropic exponent} \qquad (7b)$$

$$\rho = \rho\ (P,h,\phi) \qquad \text{thermal Equation of State (density)} \qquad (7c)$$

Frozen Mixture - The static properties are defined by

$$h = \sum_{i=1}^{Nsp} \alpha_i \quad h_i(T) \qquad \text{static enthalpy} \qquad (8a)$$

$$\gamma_f = \frac{Cp_f}{Cp_f - R/Cp_\infty} \qquad \text{ratio of specific heats and isentropic exponent } (\gamma) \qquad (8b)$$

$$Cp_f = \sum_{i=1}^{Nsp} \alpha_i \quad Cp_{i_f}(T) \qquad \text{specific heat} \qquad (8c)$$

$$w = \sum_{i=1}^{Nsp} \frac{\partial i}{m_i}^{-1} \qquad \text{molecular weight} \qquad (8d)$$

$$R = \frac{R_0}{w} \qquad \text{gas constant} \qquad (8e)$$

where pressure, temperature and density are related by

$$P = \rho \frac{R_0 T}{w} \cdot \frac{w_\infty}{\gamma_\infty M_\infty^2} \qquad \text{thermal Equation of State} \qquad (9)$$

the thermodynamic properties $Cp_i(T)$, $h_i(T)$ are tabulated polynomials, a description of which may be found in Reference (4).

C. Characteristic System - The system of Equations (1) through (6) combined with the thermodynamic system (7 or 8) yield characteristic directions for Mach numbers greater than one.

Let C_+ denote an up-running and C_- denote a down-running characteristic. Then, along a $C_{\pm}$ characteristic, whose slope is expressed by:

$$\left(\frac{dy}{dx}\right)_{\pm} = \tan(\theta \pm \mu) \tag{10}$$

the compatibility relation may be written

$$\frac{\sin\mu\cos\mu}{\Gamma} d\ln p \pm d\theta + \left(J_1\frac{\sin\theta}{y} + J_2\frac{\cos\theta}{x}\right)\frac{\sin\mu}{\cos(\theta\pm\mu)}dx = 0 \tag{11}$$

and along a streamline

$$\left(\frac{dy}{dx}\right)_s = \tan\theta \tag{12}$$

The local Mach number and Mach angle are given by

$$M = q/a \tag{13}$$

and

$$\mu = \sin^{-1}\frac{1}{M} \tag{14}$$

where

$$a^2 = \Gamma p/\rho \tag{15}$$

It should be noted that a point (x,y) in the flow, properties are completely specified by P, H, q, θ, α_i or Φ. The remaining thermodynamic variables are then determined from Equations (7 or 8)

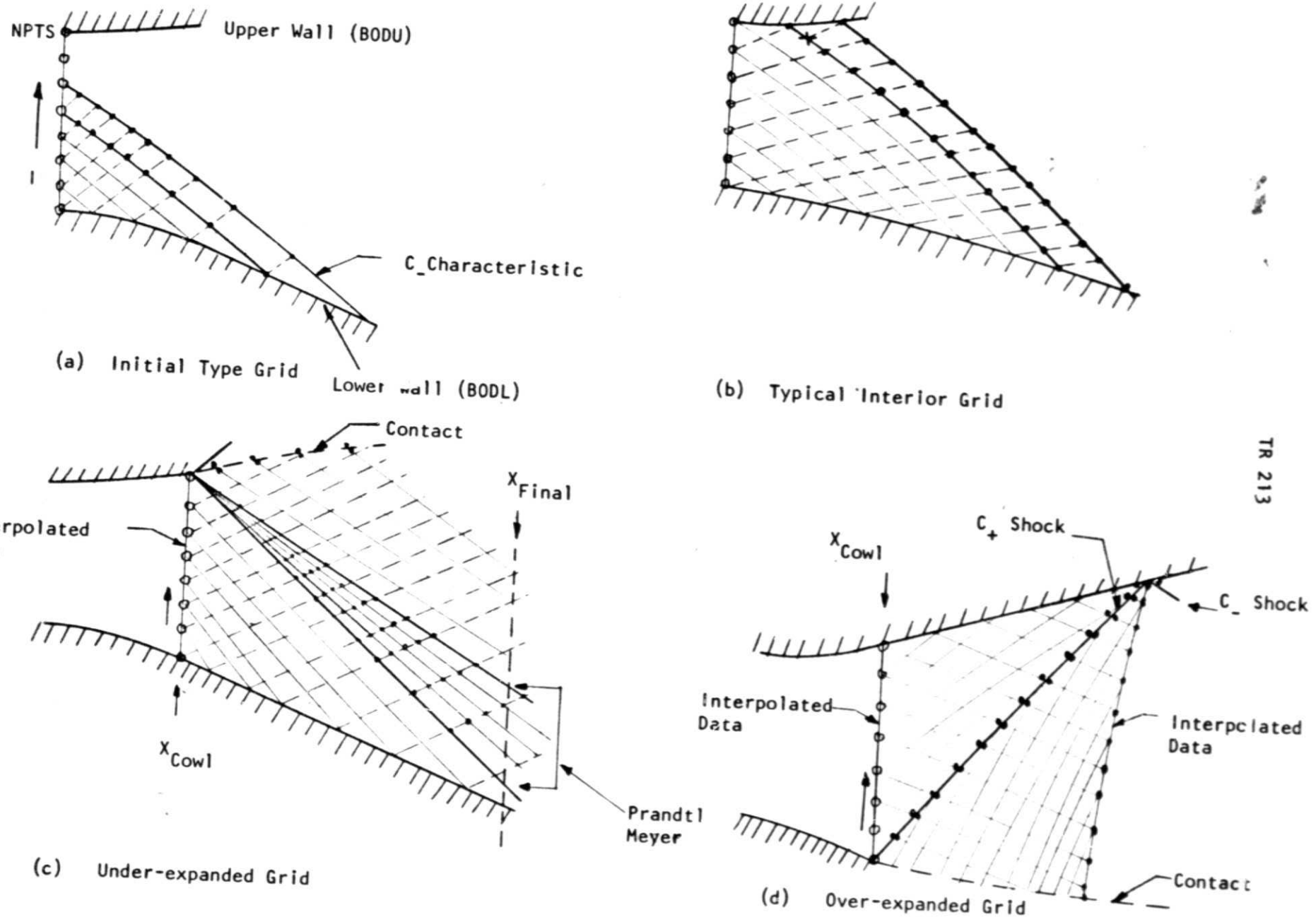

FIGURE 1. TYPICAL GRIDS

SECTION III

NUMERICAL PROCEDURE AND CHARACTERISTIC NETWORK

Figure (1) depicts the global grid ordering scheme used in the present program. While a free running characteristic network is used the program orders and stores data along down-running (C_-) characteristics (Reference 3). The only exception being the initial data line which must be a non-characteristic line. The marching proceeds from one C_- line to another until the desired flow field is calculated.

A typical characteristic mesh is depicted in Figure (2), properties being known to second order along lines EB, EA and are to be determined at the point C.

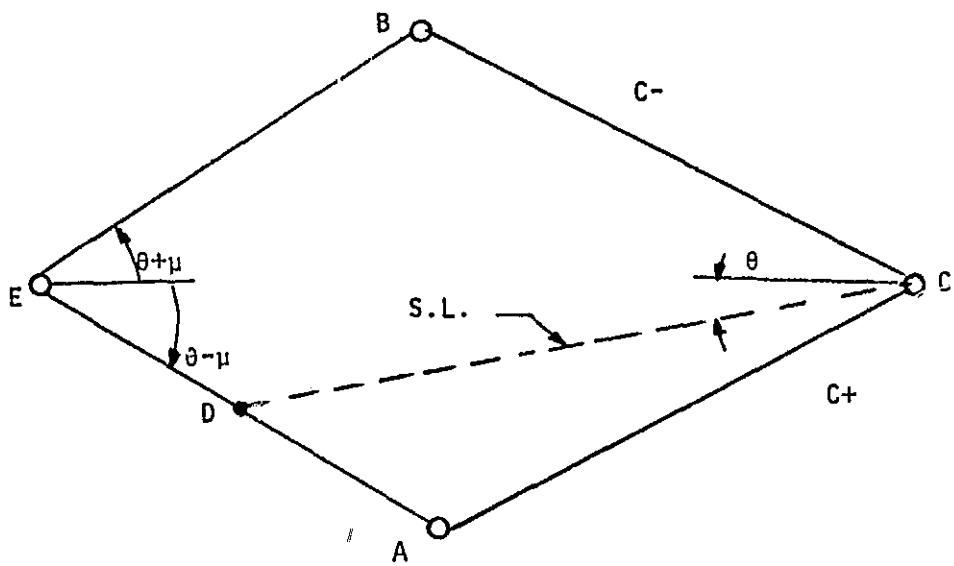

FIGURE 2. CHARACTERISTIC MESH

The location of streamline point D along characteristic EA or EB represents a significant improvement over the procedure described in Reference (3)*.

*A linear interpolation along a characteristic is second order if the properties along the characteristic are computed to second order. Appendix I contains a proof of the above statement.

For irrotational and homentropic flows the streamline location is incidental to the calculation of properties at point C. However, for highly rotational and non-homoentropic flows the streamline represents a third characteristic direction. Thus accurate representation of flow properties along streamline DC are necessary for a stable and accurate solution (Reference 5).

Let

$$G_1 = \alpha \tan(\theta+\mu)_A + \beta \tan(\theta+\xi)_C \tag{16a}$$

$$G_2 = \alpha \tan(\theta-\mu)_B + \beta \tan(\theta-\mu)_C \tag{16b}$$

and

$$G_3 = \alpha \tan \theta_D + \beta \tan \theta_C \tag{16c}$$

The Mach angles (μ) are the local values corresponding to either frozen or equilibrium flow. The α and β in the above and following equations are used as artifices in averaging properties along characteristics. In a first approximation α would be set equal to one and β equal to zero. Once properties at point C are determined, the coefficients involved in the calculation are averaged by setting both α and β equal to one-half. This corresponds to the second iteration. Writing Equation (10) in finite difference form

$$\frac{y_C-y_A}{x_C-x_A} = G_1 \tag{17a}$$

and

$$\frac{y_C-y_B}{x_C-x_B} = G_2 \tag{17b}$$

Solving the above yields

$$x_C = \frac{y_B-y_A+G_1x_A-G_2x_B}{G_1-G_2} \tag{18a}$$

$$y_C = y_A + G_1(x_C-x_A) \tag{18b}$$

$$A_1 = \alpha\left(\frac{\sin\mu\ \cos\mu}{\gamma}\right)_A + \beta\left(\frac{\sin\mu\ \cos\mu}{\gamma}\right)_C \tag{19a}$$

$$B_1 = \alpha\left(\frac{\sin\mu\ \cos\mu}{\gamma}\right)_B + \beta\left(\frac{\sin\mu\ \cos\mu}{\gamma}\right)_C \tag{19b}$$

The Mach number and angles μ are the local equilibrium or frozen values. For equilibrium flow the ratio of specific heats γ is replaced by the equilibrium exponent Γ. Similar remarks apply to all further characteristic coefficients.

$$A_2 = J_1 \left[\alpha\left(\frac{\sin\theta\ \sin\mu}{y\ \cos(\theta+\mu)}\right)_A + \beta\left(\frac{\sin\theta\ \sin\mu}{y\ \cos(\theta+\mu)}\right)_C\right] \tag{20a}$$

$$+ J_2 \left[\alpha\left(\frac{\cos\theta\ \sin\mu}{x\ \cos(\theta+\mu)}\right)_A + \beta\left(\frac{\cos\theta\ \sin\mu}{x\ \cos(\theta+\mu)}\right)_C\right] \tag{20b}$$

$$B_2 = J_1 \left[\alpha\left(\frac{\sin\theta\ \sin\mu}{y\ \cos(\theta-\mu)}\right)_B + \left(\frac{\sin\theta\ \sin\mu}{y\ \cos(\theta-\mu)}\right)_C\right] \tag{20c}$$

$$+ J_2 \left[\alpha\left(\frac{\cos\theta\ \sin\mu}{x\ \cos(\theta-\mu)}\right)_B + \left(\frac{\cos\theta\ \sin\mu}{x\ \cos(\theta-\mu)}\right)_C\right] \tag{20d}$$

Hence, along AC (C_+ characteristic)

$$A_1\ (\ln p_C - \ln p_A) + \theta_C - \theta_A + A_2\ (x_C - x_A) = 0 \tag{21a}$$

and along BC (C_- characteristic)

$$B_1\ (\ln p_C - \ln p_B) - \theta_C + \theta_B + B_2\ (x_C - x_B) = 0 \tag{21b}$$

Solving the above equations for $\ln p_C$ yields

$$\ln p_C = (A_1 \ln p_A + B_1 \ln p_B + \theta_A - \theta_B - (A_2+B_2) \; x_C + A_2 x_A + B_2 x_B)/(A_1 + B_1) \tag{22}$$

hence $p_C = \exp(\ln p_C)$ and the flow inclination is

$$\theta_C = \theta_A - A_1 \; (\ln p_C - \ln p_A) - A_2 \; (x_C - x_A) \tag{23}$$

If either the entropy or stagnation enthalpy is not constant throughout the flow field, the streamlines are the third family of characteristics, whose slope is given by

$$\frac{dy}{dx} = \tan \theta \tag{12}$$

Now, in difference form,

$$\frac{y_C - y_D}{x_C - x_D} = G_3 \tag{24a}$$

Referring to Figure (2), the point D lies between points EA or EB and can be located by an iterative procedure using Equation (24a). Properties at point D are then obtained by linearly interpolating along the appropriate characteristics EA or DB, location of point D yields the variables P_d, θ_d, $(P/\rho^{\Gamma})_d$ H_d, ρ_d, q_d, Φ_d or $\alpha_{i_d}(i=1,NSP)$.

From the streamline conservation Equations (4), (5a) or (5b) and the Equation of State (6)

$$H_C = H_D$$

$$\phi_C = \phi_D$$

or $$\alpha_{i_C} = \alpha_{i_D} \quad (i=1,NSP)$$

and $$\rho_C = (P_C(/P/\rho^{\Gamma})_D)^{1/\Gamma_C}$$

Note that as a first approximation $\Gamma_C \simeq \Gamma_D$.

If the flow is in frozen equilibrium the remaining properties at C are determined directly from

$$W_c = \left[\sum_{i=1}^{NsP} \left(\frac{\alpha i}{m_i}\right)_c \right]^{-1} ; \quad R_c = \frac{R_o}{W_c}$$

$$T_c = \left(\frac{wP}{\rho}\right)_c \cdot \frac{\gamma_\infty M_\infty^2}{w_\infty}$$

$$C_p = \sum_{i=1}^{NsP} \alpha i_c \cdot C_{p_i} (T_c)$$

$$h_c = \sum_{i=1}^{NsP} \alpha i_c \cdot h_i (T_c)$$

$$q_c = [2(H_c - h_c)]^{\frac{1}{2}}$$

$$\gamma_c = \frac{C_{p_c}}{C_{p_c} - \frac{R}{C_{p_\infty}}}$$

If the flow is in chemical equilibrium an iteration is required to determine the remaining properties at C since the temperature is obtained by inverting

the curve fit (7a) i.e., $h = h\ (P,\Phi,T)$ consistent with the density obtained from the equation of state.

Knowing the temperature T_c then yields the static enthalpy h_c. The velocity q_c is obtained from

$$q_c = [2\ (H_c - h_c)\ ]^{\frac{1}{2}}$$

and the curve fit (7b) yields

$$\Gamma_c = \Gamma\ (P,h,\Phi)$$

Equations (13), (14) and (15) then yield M_c, μ_c, a_c.

The complete calculation is then repeated with all coefficients averaged, by setting α and β equal to 1/2. If properties change significantly between these two sets of calculations, this generally implies too large a mesh in this region.

SECTION IV

BOUNDARY CALCULATIONS

The following boundary calculations are permitted in Program NOZBOD; additional details may be found in Reference (3).

A. Upper or Lower Wall - The nozzle wall shapes, either upper wall (cowl) or lower wall (vehicle undersurface) are specified by ploynomials of the form

$$y_j = A_j (x-x_i)^2 + B_j (x-x_i) + C_j \tag{25a}$$

where x_i is the origin of the wall. A maximum of 5 wall segments are permitted, i.e., $j = 5$. The wall slope θ_w is given by

$$\tan \theta_w = 2A_j (x-x_i) + B_j \tag{25b}$$

In Figure (3), DC is the specified upper nozzle wall.

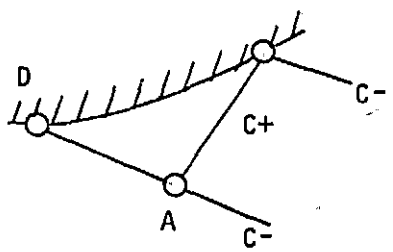

FIGURE 3. WALL POINT

Given the flow deflection (θ_w) at point C the pressure P_c is computed from the characteristic relation along AC (C+ char).

B. Shock Phenomena - The program developed has the capability of computing the shock strength associated with an inviscid supersonic over or under-expansion process, and a shock propagating into a nonuniform media.

1. Hugoniot Relations - Assume a coordinate system oriented along ($\hat{t}$ direction) and normal to the shock surface ($\hat{n}$ direction) as shown in Figure (4). The angle sigma σ is the direction cosine of the shock with respect to the Cartesian direction x, and $\tilde{u}$ and $\tilde{v}$ are the velocity components in the $\hat{n}$ and $\hat{t}$ directions.

$$\hat{n} = -\sin\sigma i_x + \cos\sigma i_y \tag{26a}$$

$$\hat{t} = \cos\sigma i_x + \sin\sigma i_y \tag{26b}$$

$$\vec{V} = \tilde{u}\hat{n} + \tilde{v}_t \hat{t} = u\hat{i}_x + v i_y \tag{27}$$

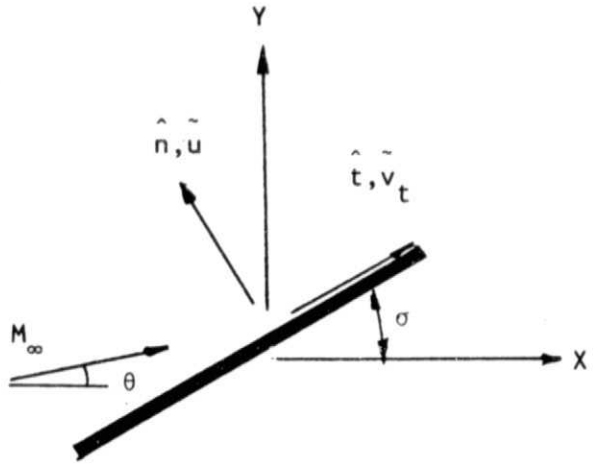

$$\hat{n} = \sin\sigma i_x + \cos\sigma i_y$$

$$\hat{t} = \cos\sigma i_x + \sin\sigma i_y$$

$$\vec{M}_\infty = M_n \hat{n} + M_t \hat{t}$$

$$\vec{M}_\infty = M_\infty(\cos\theta i_x + \sin\theta i_y)$$

FIGURE 4. SHOCK COORDINATES

The Rankin Hugoniot relations for a mixture in chemical or frozen equilibrium take the form

Continuity: $$\rho_1 \tilde{u}_1 = \rho_2 \tilde{u}_2 \tag{28}$$

Normal Momentum: $$p_1 + \rho_1 \tilde{u}_1^2 = p_2 + \rho_2 \tilde{u}_2^2 \tag{29}$$

Tangential Momentum: $$\tilde{v}_{t_1} = \tilde{v}_{t_2} \tag{30}$$

Energy: $$H = h + \frac{1}{2} V^2 = \text{constant} \tag{31}$$

State: $$\rho = \rho(p, h, \Phi_1) \qquad \text{(Equilibrium Mixture)} \tag{32a}$$

$$\rho = \frac{p_w}{R_o T} \frac{w_\infty}{\gamma M^2} \qquad \text{(Frozen Mixture)} \tag{32b}$$

where $$\Phi = \text{constant} \qquad \text{(Equilibrium Mixture)} \tag{33a}$$

$$\alpha_i = \text{constant} \qquad \text{(Frozen Mixture)} \tag{33b}$$

Employing the jump relations for a given shock angle and upstream conditions requires an iteration process since the mixture is calorically imperfect.

Let 1 designate upstream conditions and 2 downstream conditions. To solve the jump relations knowing conditions at 1, a value for $\tilde{u}_2$ is assumed. The density ρ_2 is computed using Equation (28), p_2 is computed using Equation (29) and Equation (31) yields a value for h_2. The State Equation (32) then yields an alternate value for the density. If this value for density does not agree with that calculated from continuity to within a specified tolerance, the value of u_2 is perturbed and this process is repeated until convergence is achieved.

2. Shock Point Calculation - Referring to Figure (5), a typical shock wave calculation is performed as follows. A value of the shock angle σ_C is assumed, and a simultaneous solution of the equations

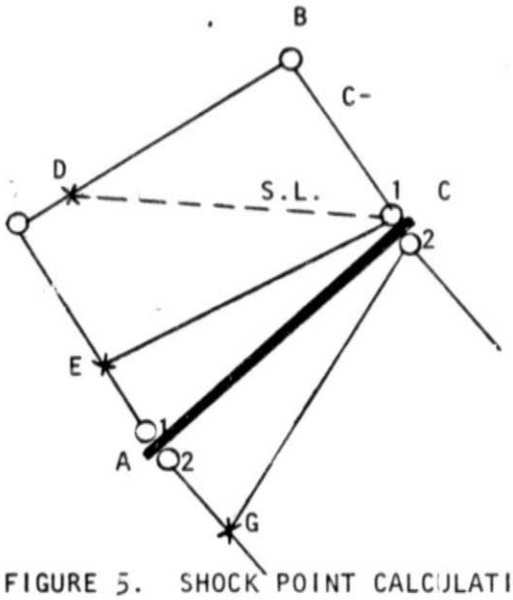

FIGURE 5. SHOCK POINT CALCULATION

$$\frac{y_C - y_{A_1}}{x_C - x_{A_1}} = \frac{1}{2} \left(\tan \sigma_C + \tan \sigma_{A_1}\right)$$

and

$$\frac{y_C - y_B}{x_C - x_B} = M_2$$

yields

$$x_C,\ y_C.$$

Since this flow is nonuniform a characteristic calculation similar to an interior point calculation yields the flow properties at C_1. Note that point E on the C_+ characteristic EC_1 is interpolated along FA_1. The jump relations (Equations 28 - 33) are solved using the determined upstream conditions based

on the assumed angle σ_C. This yields all properties at C_2. Using the deflection angle θ_{C_2} calculated from the jump conditions, a C_+ characteristic calculation performed along $(G\text{-}C_2)$ yields an alternate value of the pressure at p_{C_2}. The pressures are compared and if the difference exceeds a specified tolerance, the value of σ_C is perturbed and the process repeated until convergence is obtained. After convergence with $\alpha = 1$, $\beta = 0$, the complete calculation is repeated using $\alpha = 1/2$, $B = 1/2$.

3. Shock Reflection at Wall - The incident and reflected strength of a shock wave at a wall boundary is determined by the condition that downstream of the reflected wave (3) the flow deflection at the wall must equal the wall slope; Figure (6) depicts this interaction.

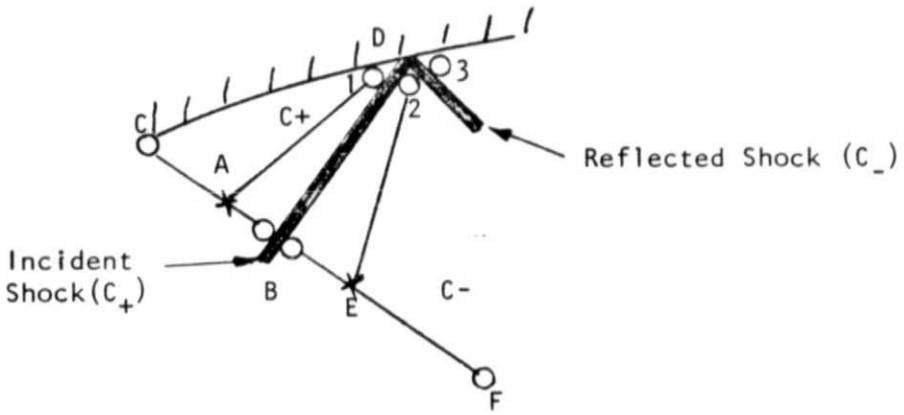

FIGURE 6. SHOCK REFLECTION AT WALL

C. Cowl Interactions

1. Under-expansion Interaction - The program developed has the capability of computing the under-expansion interaction produced by pressure mismatch between the nozzle and a surrounding airstream. This situation is depicted in Figure (7a). Under-expansion conditions occur as a result of $P_j > P_e$ or $\theta_j > \theta_e$ or some combination. Generally $P_j >> P_e$ defines an under-expanded flow.

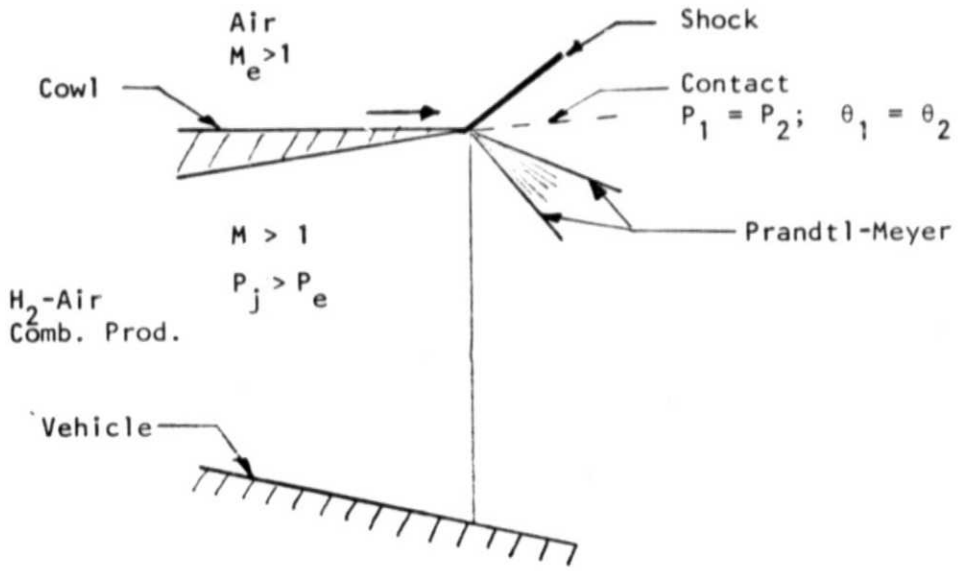

FIGURE 7a. UNDER-EXPANSION INTERACTION

2. Over-expansion Phenomena - The nozzle over-expansion at the cowl is computed in a similar fashion to the under-expanded phenomena, except that a shock wave is required in the nozzle flow and an expansion in the external flow as depicted in Figure (7b).

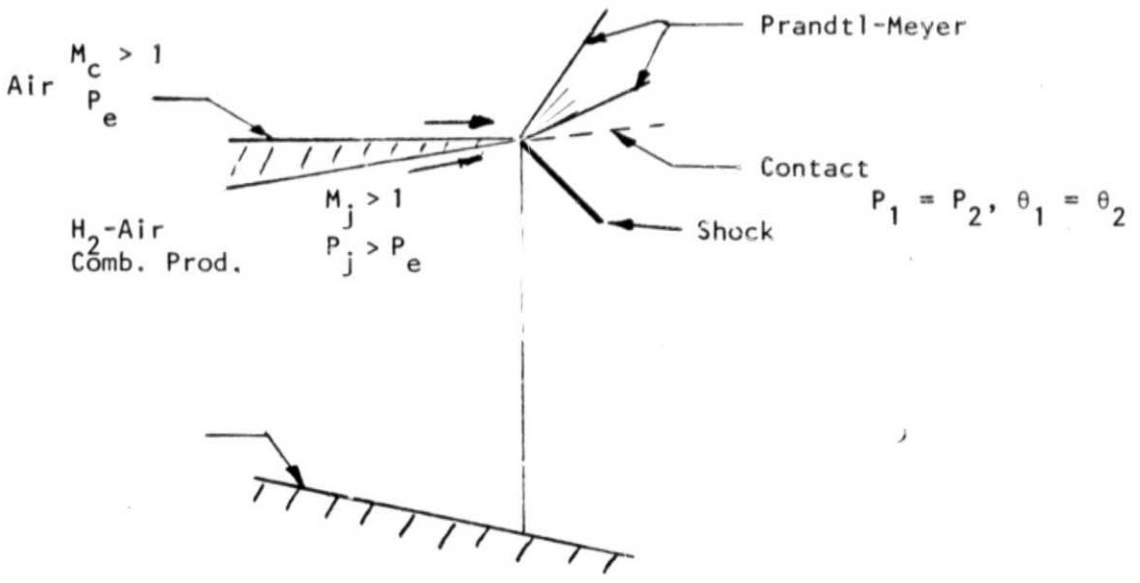

FIGURE 7b. OVER-EXPANSION INTERACTION

The jet flows are assumed to be H_2-air combustion products either in chemical or frozen equilibrium. The external flow is assumed to be a perfect gas.

D. Contact Surface - A contact surface is a stream surface of the flow, therefore, the pressure and flow deflection must be continuous across the discontinuity. Figure (8) illustrates a contact surface calculation for supersonic flow. In the present program the characteristic on the

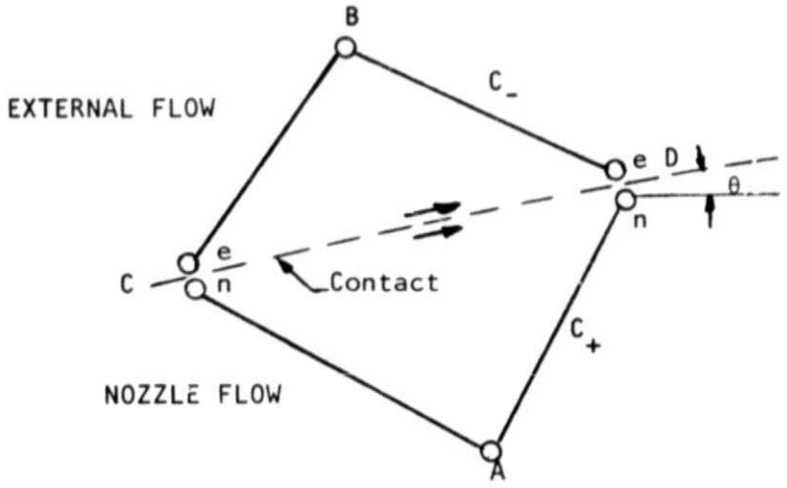

FIGURE 8. CONTACT CALCULATION

external flow side is replaced by a Prandtl-Meyer pressure-flow deflection relation or shock expansion theory and the external flow is assumed uniform. The solution requires a iterative procedure similar to a wall boundary calculation except that the shape of the boundary (i.e., contact surface) is not known a priori.

SECTION V

THRUST, LIFT AND PITCHING MOMENT

The following definitions are used in this report for thrust, lift, pitching moment

$$T = \int_A (p-p_\infty)\ \hat{i}_x \cdot d\vec{A}_n + T_{vis} \tag{34}$$

$$L = \int_A (p-p_\infty)\ \hat{i}_y \cdot d\vec{A}_n + L_{vis} \tag{35}$$

$$M_y = -\int x \cdot dL + \int y \cdot dT \tag{36}$$

Figure (9) gives the orientation of the vectors with respect to the vehicle. Internally the integrals range over all the vehicle surface areas. Externally they range over the complete vehicle undersurface as defined by the bounding stream surface and/or flow fence.

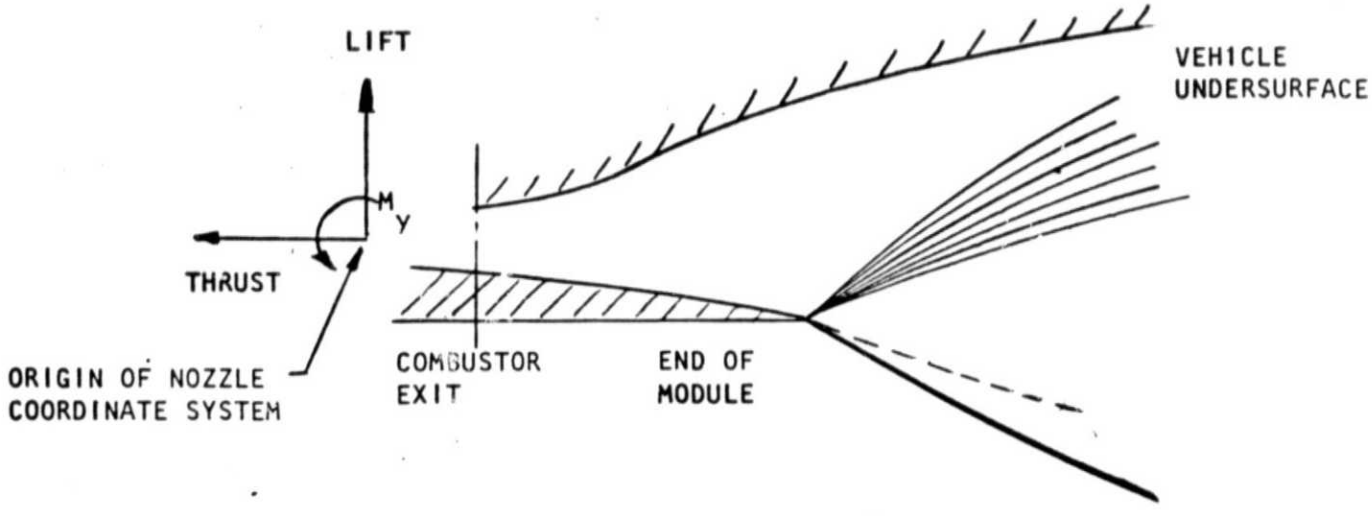

FIGURE 9. THRUST, LIFT, MOMENT

As defined above the nozzle thrust, lift and pitching may include viscous forces. These effects will be discussed below. However, we define T_{vis}, L_{vis} as

$$T_{vis} = - \int_A \left(\frac{\rho q^2}{2}\right)_{local} C_f \, \hat{i}_x \cdot d\vec{A}_s \tag{37}$$

$$L_{vis} = - \int_A \left(\frac{\rho q^2}{2}\right)_{local} C_f \, \hat{i}_y \cdot d\vec{A}_s \tag{38}$$

Surface Area Computation - Internally the nozzle surfaces are defined as the cowl internal surface, vehicle undersurface, and the nozzle sidewall. Externally the surfaces are defined as the nozzle undersurface and/or flow fences. The lateral extent of the cowl surface and nozzle undersurface is defined by the degree of lateral expansion desired.

It is assumed that the nozzle area can be approximated by a series of elemental quadrilaterals, as shown in Figure (10). From Reference (6) the unit normal for an elemental area may be obtained by defining two surface tangent vectors from the diaganols of the quadilateral.

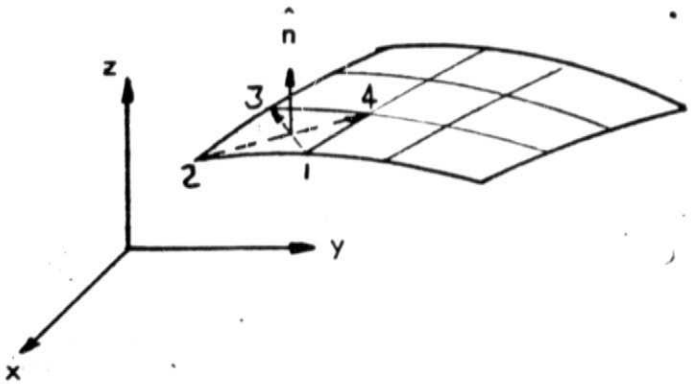

FIGURE 10. ELEMENTAL SURFACE AREA

That is

$$\vec{T}_1 = T_{1x}\,\hat{i}_x + T_{1y}\,\hat{i}_y + T_{1z}\,\hat{i}_z \tag{39a}$$

$$\vec{T}_2 = T_{2y}\,\hat{i}_x + T_{2y}\,\hat{i}_y + T_{2z}\,\hat{i}_z \tag{39b}$$

where

$$T_{1x} = x_3 - x_2, \quad T_{1y} = y_3 - y_1, \quad T_{1z} = z_3 - z_1$$

$$T_{2x} = x_4 - y_2, \quad T_{2y} = y_4 - y_2, \quad T_{2z} = z_4 - z_2$$

and the normal $\vec{N}$ is defined as

$$\vec{N} = T_2 \times T_1$$

and the unit normal as

$$\hat{n} = \frac{\vec{N}}{|\vec{N}|} \tag{40}$$

A tangent plane is constructed using the normal vector and the two tangent vectors $\overline{T}_2$, $\overline{T}_1$. The corners of the surface element are projected onto this plane and the area and centroid of the quadilateral are calculated as described in Reference (6).

Typical nozzle elemental areas are shown in Figures (11) and (12)

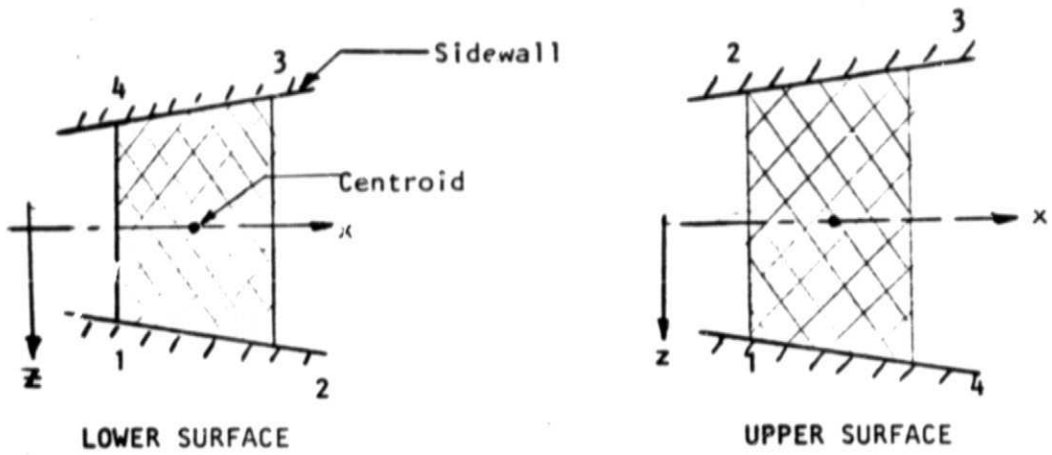

FIGURE 11. UPPER OR LOWER SURFACE AREA ELEMENTS

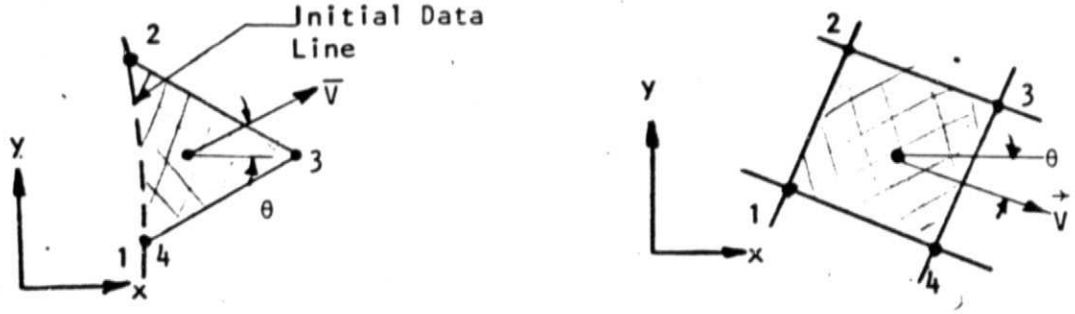

FIGURE 12. SIDEWALL AREA ELEMENTS

SECTION VI

VISCOUS EFFECTS

Local skin friction and heat transfer coefficients are computed via curve fit data supplied from Reference (6). These fits are based on the Spalding and Chi method of Reference (7). That is a suitably transformed skin-friction coefficient is given by incompressible formulas based on a suitably transformed Reynolds number, i.e.:

$$C_{f_\delta} = C_{f_i}/F_c \tag{41}$$

$$C_{f_i} = f(Rx_i), \quad Rx_i = F_{Rx} \cdot Rx \tag{42}$$

where

C_f = local skin friction coefficient

Rx = Reynolds number

$( )_i$ = indicates incompressible

$( )_\delta$ = indicates compressible

Now for $Rx_i > 2540$ the local skin friction is given from Reference (8) as

$$C_{f_i} = .088\ (\log Rx_i - 2.3686)/(\log Rx_i - 1.5)^3 \tag{43}$$

and from Reference (5)

$$F_c = A/\left[\ \text{ARSIN}\ \left(\frac{A-B}{C}\right) + \text{ARSIN}\ \left(\frac{A+B}{C}\right)\right]^2 \tag{44}$$

$$A = \frac{H_{AW}}{H_\delta} - 1 \tag{45a}$$

$$B = \frac{H_W}{H_\delta} - 1 \tag{45b}$$

$$C = \left[(A+B)^2 + 4A \right]^{1/2} \tag{45c}$$

$$F_{Rx} = \left(\frac{H_{AW}}{H_\delta}\right)^q \Big/ \left[F_c \left(\frac{H_W}{H_\delta}\right) \right]^{p+q} \quad , q = 0.772, \; p = 0.702 \tag{46}$$

The local properties external to the boundary layer are the local data computed by NOZBOD and are assumed to act through the centroid of the element area computed above. The computation requires that a boundary layer origin be specified since the nozzle is assumed to be an extension of the combustor. In addition a recovery factor for an adiabatic wall calculation is required. However, as a user option wall temperature distributions may be specified.

Local heat transfer coefficients are computed from a modified Reynolds analogy for turbulent flow

$$St = Sh \cdot C_f/2 \tag{47}$$

The program requires "Sh" as an input item.

SECTION VII

CHARACTERISTIC COALESCENCE

Since the program developed stores data on c^- characteristics, shock wave detection for both first and second family shocks is straight forward. A shock wave is present if two characteristics of the same family intersect each other within the flow field.

While characteristic crossings are detected automatically the program does not insert shock waves into the flow field calculation. However, by judiciously eliminating data points and noting these locations an approximate shock wave trace may be obtained during the course of the calculation.

For down-running shocks, detection must take place prior to the calculation of a new data point. Figure (13) illustrates the procedure. Since the flow

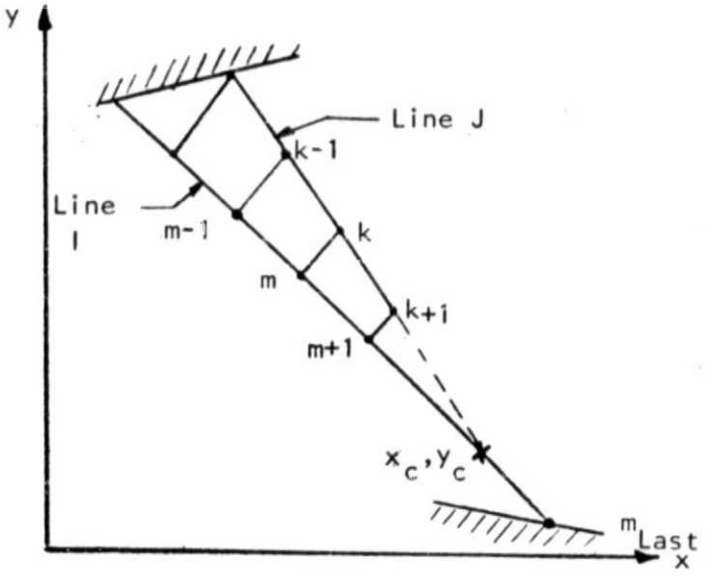

FIGURE 13. DOWN-RUNNING (c^-) SHOCK DETECTION

field is known on Line 1, and up to point K on Line J, and if point K+1 is the next data point to be calculated, a crossing of c^- characteristics may be determined from the following relations.

$$(y_c - y_k)_j = M \cdot (x_c - x_k)_j$$

$$(y_c - y_m)_1 = N \cdot (x_c - x_m)_1$$

where

$$M = \frac{y_k - y_{k-1}}{x_k - x_{k-1}}$$

and

$$N = \frac{y_m - y_{m-1}}{x_m - x_{m-1}}$$

If $x_c > x_k$ then the initial shock strength is related to the relative distance $(S_c - S_k)/\Delta S_t)$ where S is the running distance along the c^- characteristic and ΔS_t is an average mesh distance on Line 1. If the above ratio is less than a given tolerance no further data on Line J is calculated and the new initial data line becomes Line J up to point K and the remainder of Line 1 from m+1 to m_{last}. A new data line is calculated from this hybrid data and the process repeated.

Detection of up-running shocks may be accomplished after completing the calculation of new data Line J. Figure (14) is an illustration of the process. The crossing of c^+ characteristics may be obtained from the following relations

$$(y_c - y_k) = M \cdot (x_c - y_k)$$

$$(y_c - y_{k+1}) = N \cdot (x_c - x_{k+1})$$

where

$$M = \frac{y_{k+1} - y_{m+1}}{x_{k+1} - x_{m+1}}$$

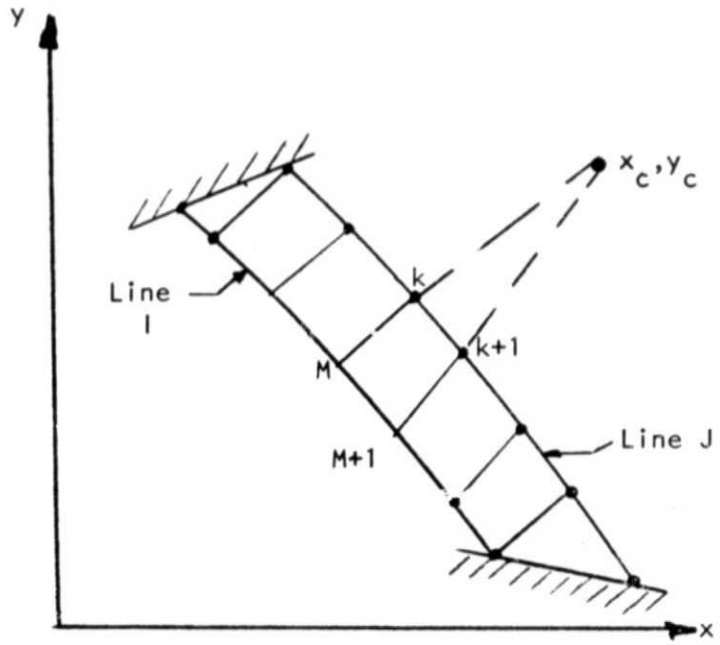

FIGURE 14. UP-RUNNING (c^+) SHOCK DETECTION

and

$$N = \frac{y_k - y_m}{x_k - x_m}$$

The up-running (c^+) initial shock strength is determined by the relative distance $(x_c - x_k)/(x_k - x_m)$. If the above ratio is less than a given tolerance, the point k+1 is dropped from the data Line J and the next data line is calculated using Line J minus point k+1.

Thus, a continuous trace of both up-running and down-running shock waves may be obtained. It should be noted that the process of dropping selective data points is valid only for shock waves which do not appreciably alter the flow field entropy distribution.

SECTION VIII

SUMMARY AND CONCLUSION

In Reference (3) a unique characteristic procedure was developed which computes realistic scramjet nozzle exhaust flow fields, using an axially expanding coordinate system (line source) allowing lateral nozzle area variations to be accounted for in a quasi two dimensional fashion. Additional geometric flexibility was incorporated in the numerical procedure through the use of additional coordinate systems i.e., axisymmetric and Cartesian. The technique is second order in a characteristic sense.

The present study reported herein extends and improves upon the authors previous work. Improved streamline interpolation procedures insure numerical stability and improve program accuracy. The extension of the present work to include plume shape affects on vehicle forces removes a major shortcoming of the previous work. In addition, sophisticated force and moment calculations allows for accurate incorporation of sidewall/fence forces and viscous effects (internal drag and heat transfer). Thus heat transfer effects can be used to assess vehicle structural and weight considerations. Shock detection techniques have been incorporated so as to accurately determine where body shapes should be modified in order to allow shock free flow.

Thus, it is felt that the current program will give the designer of scramjet nozzle exhaust flow fields increased flexibility not previously available.

REFERENCES

1. Ferri, A, Dash, S. and Del Guidice, P., "Methodology for Three Dimensional Nozzle Design," ATL TR 195, (NASA CR 132438), March 1974.

2. Dash, S. and Del Guidice, P., "A Numerical Procedure for the Parametric Optimization of Three Dimensional Scramjet Nozzles," ATL TR-188, (NASA CR-132440), October 1973.

3. Del Guidice, P., Dash, S. and Kalben, P., "A Source Flow Characteristic Technique for the Analysis of Scramjet Exhaust Flow Fields," ATL TR 186, (NASA CR 132437), March 1974.

4. McBride, B.J., Heimel, S., Ehlers, J.G. and Gordon, S., "Thermodynamic Properties to 6000^{o}K for 210 Substences Involving the First 18 Elements," NASA SP-3001, (1963).

5. Sedney, R., "The Method of Characteristics," Non-Equilibrium Flows, Part II, Marcel Dekker Inc., New York (1970).

6. Gentry, A.E. and Smyth, D.N., "Hypersonic Arbitrary-Body Aerodynamic Computer Program, Mark II Version" Vol. II, Douglas Report DAC 61552, April 1968.

7. Spalding, D.B. and chi, S.W., "Drag of a Compressible Turbulent Boundary Layer on a Smooth Flat Plate With and Without Heat Transfer," J. Fluid Mechanics, Vol. 18, Pt. 1, January 1964.

8. Sivells, J.C. and Payne, R.G., "A Method of Calculating Turbulent Boundary Layer Growth at Hypersonic Mach Numbers," AEDC TR 59-3, March 1959.

9. Ferri, A.,"The Method of Characteristics," Section G of The General Theory of High Speed Aerodynamics, Vol. VI, Princeton University Press, (1954).

APPENDIX

Linear Interpolation on Characteristics

A Second Order Procedure

Employing a linear interpolation procedure ona characteristic line calculated to second order is consistent with a second order algorithm. This point can be inferred from Ferri's article in Vol. 6 of the Princeton series but apparently, is not universally accepted (i.e., Reference 5). Hence, a simple proof of this statement is presented.

Along any line AC, a series expansion for the pressure and flow deflection are written:

$$P_C = P_A + (P_x)_A \Delta x_{AC} + (P_{xx})_A (\Delta x^2/2)_{AC} + 0 (\Delta x^3)_{AC} \tag{A1}$$

$$\theta_C = \theta_A + (\theta_x)_A \Delta x_{AC} + (\theta_{xx})_A (\Delta x^2/2)_{AC} + 0 (\Delta x^3)_{AC} \tag{A2}$$

but

$$(P_x)_C = (P_x)_A + (P_{xx})_A \Delta x_{AC} + 0 (\Delta x^2)_{AC} \tag{A3}$$

$$(\theta_x)_C = (\theta_x)_A + (\theta_{xx})_A \Delta x_{AC} + 0 (\Delta x^2)_{AC} \tag{A4}$$

(where x denotes distance along AC).

Substituting (3) into (1) and (4) into (2) we obtain

$$P_C = P_A + [(P_x)_A + (P_x)]_C (\Delta x/2)_{AC} + 0 (\Delta x^3)_{AC} \tag{A5}$$

$$\theta_C = \theta_A + [(\theta_x)_A + (\theta_x)]_C (\Delta x/2)_{AC} + 0 (\Delta x^3)_{AC} \tag{A6}$$

The above expressions are valid along any line AC. Now at points A and C, we write the compatibility relations, assuming that AC is a downrunning characteristic.

$$(\theta_x)_A - A_A (P_x)_A = 0 \tag{A7}$$

$$(\theta_x)_C - A_C (P_x)_C = 0 \tag{A8}$$

Solving the system (5) - (8) for $(P_x)_A + (P_x)_C$, we obtain

$$(P_x)_A = \frac{-2}{\Delta x(A_C - A_A)} (\theta_C - \theta_A) - A_C (P_C - P_A) \tag{A9}$$

and

$$(P_x)_C = \frac{2}{\Delta x(A_C - A_A)} (\theta_C - \theta_A) - A_A (P_C - P_A) \tag{A10}$$

Now consider a point x^* between A and C. The pressure at this point, to second order is given by

$$P^* = P_A + (P_x)_A (x^* - x)_A + \frac{(Px)_C - (Px)_A}{\Delta x_{AC}} (x^* - x)_A^2 + 0(\Delta x^3) \tag{A11}$$

where $(P_x)_A$ and (P_x) are given by (9) and (10). Till this point, all relations are quite general and have not required that a second order compatibility relation exist between A and C. We now make use of this relation by stating that by second order, we imply that the relation

$$(\theta_C - \theta_A) - \left(\frac{A_A + A_C}{2}\right) (P_C - P_A) = 0 \tag{A12}$$

is satisfied between points A and C in a convergent fashion as detailed in Reference (9). Then, substituting Equation (12) into Equations (9) and (10) we obtain:

$$(P_x)_C - (P_x)_A = 0 \tag{A13}$$

and

$$(P_x)_A = \frac{(P_C - P_A)}{(X_C - X_A)} \tag{A14}$$

Hence, substituting these relations into Equation (11) yields

$$P^* = P_A + (P_C - P_A) \frac{(X^* - X_A)}{(X_C - X_A)} + 0 \quad (\Delta x^3)$$

which clearly demonstrates that a linear interpolation for pressure (or flow deflection) on a characteristic calculated to second order is consistent with a fully second order approach.